Structural Engineering and Mechanics, Vol. 45, No. 6 (2013) 821-835
DOI: http://dx.doi.org/10.12989/sem.2013.45.6.821

An improvement to seismic design of substation support structures

Reza Karami Mohammadi[*1], Vahid Akrami[2a] and Farzad Nikfar[3b]

[1]Civil Engineering Department, K. N. Toosi University of Technology (KNTU), Tehran, Iran
[2]Civil Engineering Department, Amirkabir University of Technology, Tehran, Iran
[3]Civil Engineering Department, McMaster University, Hamilton, Canada

(Received August 18, 2011, Revised January 15, 2013, Accepted February 23, 2013)

Abstract. The acceleration that the electrical equipment experiences on a structure can be several times the ground acceleration. Currently, substation support structures are being designed according to ASCE (Substation Structure Design Guide 2008), without any consideration about effects of these structures on dynamic behavior of mounted equipment. In this paper, a parametric study is implemented in order to improve seismic design of candlestick substation structures based on this design guide. To do this, dynamic amplification factor (DAF) of different candlestick support-equipment combinations is evaluated and compared to the target DAF presented in IEEE STD 693 (2006). Based on this procedure, a new criterion is developed to restrict maximum acceleration at support-equipment intersection.

Keywords: seismic design; dynamic amplification factor; substations; support structures

1. Introduction

As an important part of lifeline systems, electrical power system plays a vital role in a country, and its safety problems affect the construction quality and the daily life of ordinary people directly. Recent moderate and strong earthquakes happened all over the world, have demonstrated that parts of electric power systems are very vulnerable to damage (ASCE Manual 1996, ASCE-TCLEE 1997, AIJ Report 1998). These earthquake induced damages to substation components will degrade the power network performance, potentially leading to a network blackout (Shinozuka *et al*. 2007, Chang and Wu 2011).

Many different parameters can affect seismic behaviour of substation equipment; however, performance is strongly influenced by specific equipment design and installation practice. One of the important parameters affecting seismic performance of any substation equipment is the dynamic properties of supporting structure (Hatami *et al*. 2004, Wen and Niu 2011). According to recommendations of IEEE STD 693 (2006), substation support structures should be designed using ASCE Manual (2008). Although this design guide seems to be a good reference for design of

*Corresponding author, Assistant Professor, E-mail: rkarami@kntu.ac.ir
[a]Ph.D. Student, E-mail: v.akrami@aut.ac.ir
[b]Ph.D. Student, E-mail: nikfarf@mcmaster.ca

substation structures, but in some cases its procedure implemented to seismic design of supporting structures can be discussed and improved.

Evaluation of dynamic amplification factor (DAF) at support-equipment intersection is one of these cases which are not considered in ASCE design guide. Knowing that the substation support structures should be quite tall in order to provide the needed electrical clearance and ensure personnel safety, it can be said that these structures amplify ground motions during an earthquake event. Generally, the acceleration that the substation equipment experiences on a structure can be several times the ground acceleration. If the dynamic amplification of supporting structure is not controlled during the design of structure, it may cause the failure of mounted equipment due to the excessive acceleration which is induced by the supporting structure. Based on IEEE STD 693 (2006), during seismic qualification, it is generally desirable to have the equipment mounted or modeled in the identical manner as it would be in its in-service configuration. However, for different reasons it is not practical to qualify the equipment in its in-service configuration. For these equipment types the qualification should be done without supporting structure at 2.5 times the specified requirements by IEEE STD 693. Accordingly, the users shall design the structures such that the supports do not amplify the base accelerations more than 2.25 times. Nevertheless, there is not any recommendation in ASCE design guide, in order to restrict the maximum base acceleration of equipment to this specified criterion.

The importance of the problem will be more highlighted considering the fact that most of the substation equipment items are often highly interconnected with neighbouring components. The necessity of considering dynamic effects of supporting structure on seismic behaviour of such interconnected systems is confirmed in some studies (Dastous *et al*. 2004, Dastous 2007, Dastous and Pierre 2007). Dynamic amplification of substation structures is studied by different researchers. Among the rest, Gilani *et al*. (2000), studied the effects of different supports with different heights and stiffness on the seismic behavior of 230kV disconnect switches. Amplification factors of 2 - 3 were reported for structures studied in this report. Although the amplification factor of one of studied structures was in excess of 3 which indicates that the mounted equipment should resist accelerations more than three times the peak ground acceleration (PGA). In a similar research Takhirov *et al*. (2004), studied the seismic behavior of 550kV disconnect switches through fragility testing. Some other researchers (Matt and Filiatrault 2004, Pham 2005, Feizi *et al*. 2008) studied the spectral amplification of different transformer tanks and their effects on seismic behavior of bushings.

In this research, a parametric study is implemented in order to improve seismic design of substation support structures (especially candlestick ones) based on recommendations of IEEE STD 693 and ASCE design guide. To do this, dynamic amplification of different candlestick support-equipment sets is calculated at support-equipment intersection and compared to the target DAF proposed by IEEE STD 693 (i.e., 2.25). Using this method, a minimum stiffness ratio is proposed for different combinations of supports and equipment which is required in order to have a DAF smaller than 2.25. Effect of different top and bottom masses on DAF of supporting structure is also studied in this section.

Generally speaking, DAF of a support-equipment system with specified properties is not a unique quantity and it depends on the spectral shape of the earthquake used to calculate DAF. In other words, a support-equipment system which its DAF is calculated using a specific response spectrum may have a different DAF when subjected to another earthquake. In the closing part of this study, an introductory discussion is done about probabilistic evaluation of DAF. Based on the results, for a support-equipment system which its DAF is controlled using the minimum stiffness ratios proposed in this paper, there will be only about 4-9% probability of not being qualified Using IEEE STD 693 specifications. Results of this study can be utilized in order to better design and control of candlestick substation support structures. Implementing the proposed method in conjunction with a seismic design code, e.g., ASCE (Substation Structures Design Guide) can result in more robust structures and decreases earthquake damages to electrical equipment.

2. Modeling and assumptions

For candlestick support-equipment systems, the electrical equipment and its supporting structure can be modeled as a 4DOF system (Fig. 1). The illustrated model is composed of two beam elements with distributed mass and constant material properties, e.g. bending stiffness. In this figure, EI_s, L_s and $\bar{m}_s$ are bending stiffness, length and distributed mass of supporting structure, respectively. EI_e, L_e and $\bar{m}_e$ are the same quantities corresponding to the mounted equipment.

Two concentrated masses, namely M_b and M_t are representative of dead and live tank masses installed at top or bottom of equipment, respectively. It should be noted that for most equipment types such as CTs, CVTs, PIs and other equipment with negligible tank mass, the value of M_t and M_b can set to be zero.

Using the consistent mass and stiffness matrices of Euler beam element (Clough and Penzien 1993), the consistent mass and stiffness matrices of entire system can be written as

$$M=\frac{156\bar{m}_e L_e}{420}\begin{bmatrix} \alpha_m\alpha_L+1+\frac{420\gamma_b}{156} & \frac{9}{26} & \frac{11(1-\alpha_m\alpha_L{}^2)L_e}{78} & -\frac{L_e}{12} \\ \frac{9}{26} & 1+\frac{420\gamma_t}{156} & \frac{L_e}{12} & -\frac{11L_e}{78} \\ \frac{11(1-\alpha_m\alpha_L{}^2)L_e}{78} & \frac{L_e}{12} & \frac{(1+\alpha_m\alpha_L{}^3)L_e^2}{39} & -\frac{L_e^2}{52} \\ -\frac{L_e}{12} & -\frac{11L_e}{78} & -\frac{L_e^2}{52} & \frac{L_e^2}{39} \end{bmatrix} \tag{1}$$

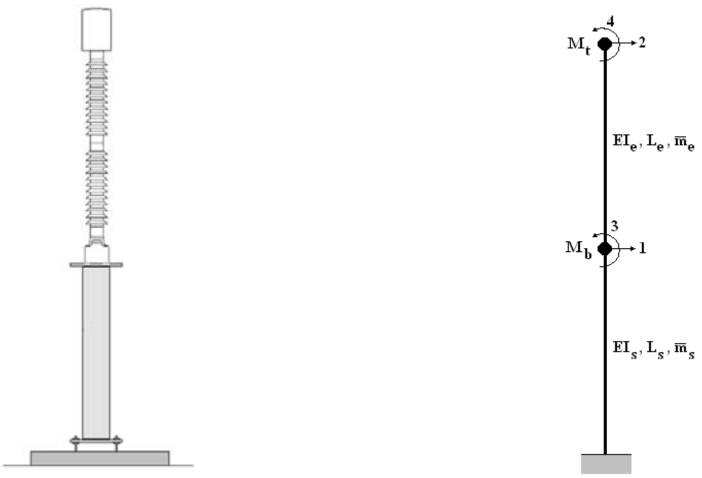

Fig. 1 Example of electrical equipment and corresponding 4DOF model

$$K = \frac{2EI_e}{L_e^3}\begin{bmatrix} 6\frac{\alpha_{EI}+\alpha_L^{\,3}}{\alpha_L^{\,3}} & -6 & 3\frac{\alpha_L^{\,2}-\alpha_{EI}}{\alpha_L^{\,2}}L_e & 3L_e \\ -6 & 6 & -3L_e & -3L_e \\ 3\frac{\alpha_L^{\,2}-\alpha_{EI}}{\alpha_L^{\,2}}L_e & -3L_e & 2\frac{\alpha_{EI}+\alpha_L}{\alpha_L}L_e^2 & L_e^2 \\ 3L_e & -3L_e & L_e^2 & 2L_e^2 \end{bmatrix} \tag{2}$$

Where:

$$\alpha_m = \frac{\bar{m}_s}{\bar{m}_e}, \quad \alpha_{EI} = \frac{EI_s}{EI_e}, \quad \alpha_L = \frac{L_s}{L_e}, \quad \gamma_b = \frac{M_b}{\bar{m}_e L_e}, \quad \gamma_t = \frac{M_t}{\bar{m}_e L_e}$$

Parameters of this model (i.e., height, mass and stiffness) should be rationally adjusted to the actual support-equipment system. For support structures with standard cross section, the value of EI_s can be calculated easily. However, for other types of supporting structures, e.g., latticed structures, this value should be calculated using a structural analysis. For some substation equipment the value of EI_e can be found in equipment technical specification. But it should be noted that the parameter EI_e is not a commonly used quantity and hence is not usually addressed in equipment technical specifications. Using the equation presented for natural frequency of a continuous beam element with distributed mass and constant material properties (Clough and Penzien 1993, Chopra 2007), the value of this parameter can be calculated from following equation

$$EI_e = \frac{\bar{m}_e L_e^4 \omega_e^2}{\lambda_e} \tag{3}$$

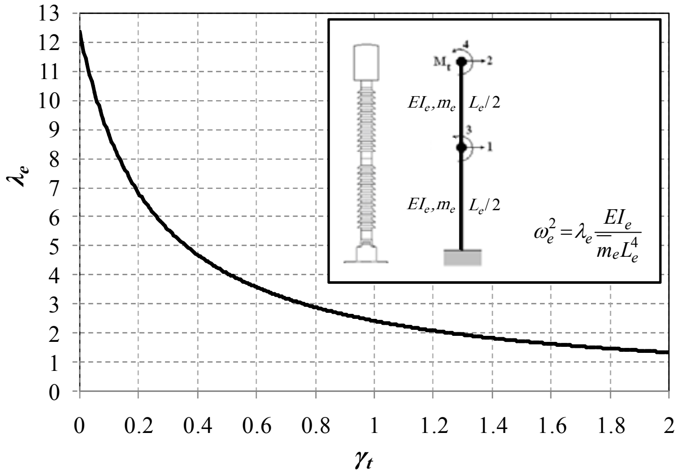

Fig. 2 Value of λ_e For different top masses

Where the parameters $\bar{m}_e$, L_e, and ω_e (natural frequency of equipment) are well-known quantities which can be found easily in any equipment technical specification. The value of λ_e for a candlestick equipment set without top mass, $\gamma_t = 0$, (a continuous beam element with distributed mass and constant material properties) can be found in different references such as Clough and

Penzien (1993) or Chopra (2007). For equipment sets with various top masses this parameter can be calculated using the simplified 4DOF system shown in Fig. 2. For the support-equipment system shown in this figure, the fundamental natural frequency can be computed using the mass and stiffness matrices given in Eqs. (1) and (2) just by substituting L_e with $L_e/2$ and setting $\alpha_m = 1.0$, $\alpha_{EI} = 1.0$, $\alpha_L = 1.0$ and $\gamma_b = 1.0$. Solving the eigen value problem for this simplified parametric model the value of λ_e is obtained for different top masses and presented in Fig. 2.

3. Evaluation of DAF

As it was mentioned before, the acceleration that the equipment experiences on a structure can be several times the ground acceleration. In this section it is intended to establish a new criterion in order to control DAF of supporting structures.

Having determined the value of different modal frequencies, mode shapes corresponding to each frequency can be calculated using a modal analysis. The modal participation factor corresponding to DOF j, and vibration mode n, may be indicated as (Chopra 2007)

$$D_{jn} = \phi_{jn} \frac{[\Phi]_n^T [M] i}{[\Phi]_n^T [M][\Phi]_n} \tag{4}$$

Where, i, is the influence vector as defined in (Chopra 2007) and ϕ_{jn} is the mode shape corresponding to j^{th} DOF and n^{th} vibration mode. The absolute acceleration at support-equipment intersection (first DOF) corresponding to each vibration mode can be calculated as follows

$$A_{1n} = D_{1n} \times Sa(\omega_n, \xi) \tag{5}$$

In this equation, $S_a(\omega_n, \xi)$ is the spectral acceleration which defines the response of a single degree of freedom (SDOF) system with natural frequency of ω_n and damping ratio of ξ. The value of dynamic amplification factor at support-equipment intersection can be computed using an appropriate combination method of the modal responses. Usually, different combination methods are used for modal superposition of responses. In this paper, modal responses are combined using absolute sum method which is conservative and is the preferred combination method recommended by IEEE STD 693. Using this method, dynamic amplification factor of supporting structure can be computed as

$$DAF = \sum_{n=1}^{N} \left| D_{1n} \times B(\omega_n, \xi) \right| \tag{6}$$

Where, N, is number of DOFs, ξ, is damping ratio which can be assumed to be 2% of critical damping (as recommended by IEEE STD 693) and $B(\omega_n, \xi)$ is the value of response spectrum normalized by PGA.

As it was mentioned before, according to specifications of IEEE STD 693, when an equipment qualification is being done without supporting structure, the resulting DAF obtained from Eq. (6) should be less than 2.25 when the support-equipment system is exposed to required response spectrum (RRS). Using either high or moderate RRS of IEEE STD 693, the value of normalized response spectrum to be used in Eq. (6) shall be taken as

$$\begin{aligned}
&B(\omega_n,\xi)=\frac{1.144\beta\omega_n}{\pi} && 0.0\le\omega_n\le 2.2\pi \\
&B(\omega_n,\xi)=2.5\beta && 2.2\pi\le\omega_n\le 16\pi \\
&B(\omega_n,\xi)=\frac{2\pi(26.4\beta-10.56)}{\omega_n}-0.8\beta+1.32 && 16\pi\le\omega_n\le 66\pi \\
&B(\omega_n,\xi)=1 && \omega_n\ge 66\pi
\end{aligned} \tag{7}$$

Where

$$\beta=\frac{(3.21-0.68\ln(\xi))}{2.1156} \tag{8}$$

It should be noted that both high and moderate response spectra presented in IEEE STD 693, have the same spectral shape which is shown in Fig. 3.

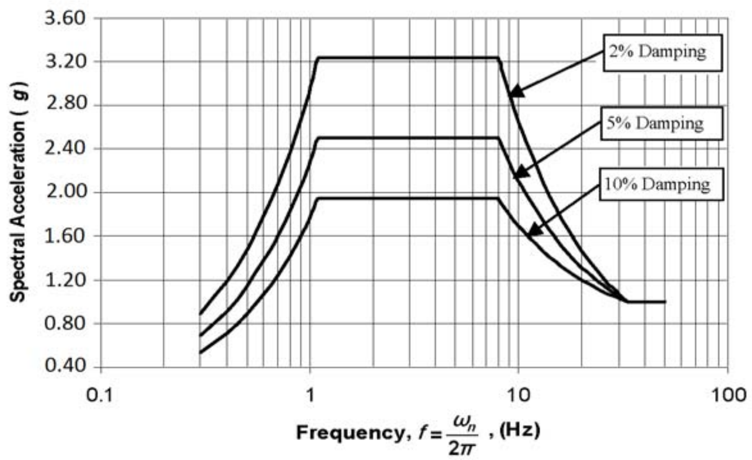

Fig. 3 Normalized response spectrum of IEEE STD 693 (2006)

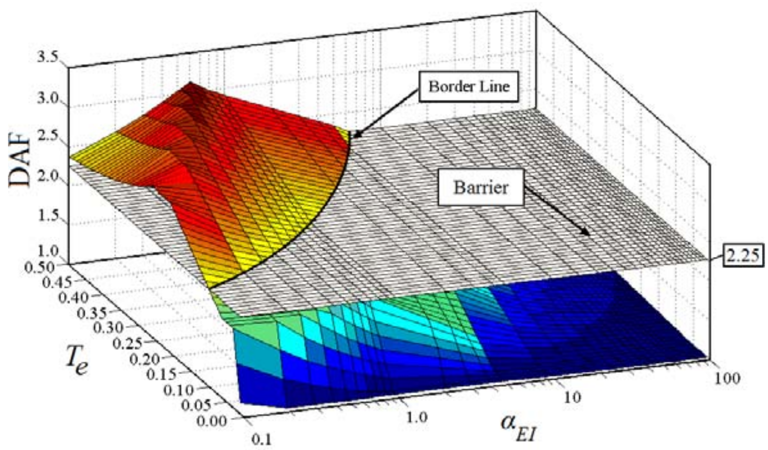

Fig. 4 DAF of a substation structure in which $\alpha_m = \alpha_L = 0.8$

3.1 Equipment without top and bottom masses

In this part, DAF of substation structures is calculated for different candlestick support-equipment sets and checked to be less than target DAF presented in IEEE STD 693.

Using Eq. (6), DAFs for a support-equipment system with mass and height ratios equal to 0.8 ($\alpha_m = \alpha_L = 0.8$) are calculated and shown in Fig. 4. Two horizontal axes are representative of system stiffness ratio (α_{EI}) and equipment natural period (T_e). Corresponding values of DAF is represented in the vertical axis. As it was anticipated, DAF of supporting structure tends to unity as the value of stiffness ratio increases. The gray surface shown in this figure corresponds to the target DAF recommended by IEEE STD 693 (DAF = 2.25). According to this figure, the value of DAF for some (α_{EI}, T_e) combinations is above the target DAF. The curve obtained from intersection of two surfaces will result in a border line between acceptable and unacceptable DAFs.

Considering the border line shown in Fig. 4, a minimum stiffness ratio, $(\alpha_{EI})_{\min}$, can be found which is required by support-equipment system in order to have a DAF smaller than 2.25. The minimum bending stiffness of supporting structure, EI_s, may be calculated accordingly

$$EI_s \geq (\alpha_{EI})_{\min} EI_e \tag{9}$$

Substituting Eq. (3) in Eq. (9), one can write

$$EI_s \geq (\alpha_{EI})_{\min} \frac{\overline{m}_e L_e^4 \omega_e^2}{\lambda_e} \tag{10}$$

In above expression, $\overline{m}_e$ is distributed mass of equipment in (kg/m), L_e is the height of equipment in (m) and EI_s is the minimum allowable bending stiffness of supporting structure in (N.m^2). λ_e can be obtained from Fig. 2.

As an example, consider a capacitive voltage transformer (CVT) with given properties: $L_e =$ 4.65m, $\overline{m}_e L_e =$ 750kg and $T_e =$ 0.18sec ($\gamma_b = \gamma_t = 0$). Also assume that from seismic design of supporting structure we have: $\alpha_m = \alpha_L = 0.8$. Based on calculations, the minimum stiffness ratio for this system will be equal to 3.74 which results in $EI_s \geq$ 27802 kN.m^2. Using a steel tubular section (with modulus of elasticity, $E = 2.1\times10^6$kg/cm^2) with wall thickness equal to 0.5cm, the minimum outer diameter of supporting structure will be equal to 51.8 cm. Hence, the seismic design of this supporting structure will be acceptable if the diameter of designed section is greater than 51.8cm.

Above example indicates a special case which may be rarely found in actual practice. For other candlestick support-equipment systems with various mass and height ratios, different border lines can be found between safe and unsafe states as shown in Fig. 5. According to Fig. 5(a), for special equipment, as the height of structure decreases the required stiffness ratio decreases in order to pass IEEE STD 693 criterion. To see effect of height ratio, consider the previous example with α_m = 0.8 and α_L = 0.4. For this support-equipment combination the minimum stiffness ratio will be equal to 0.14 which results in a minimum support diameter equal to 17.5cm. In a similar manner, as the natural period of equipment decreases, the required stiffness ratio of system decreases too.

As it can be inferred from Fig. 5(b), there is a similar trend for various mass ratios, however the changes in minimum stiffness ratio due to variation of parameter α_L is more evident than the changes due to variation of parameter α_m. Again, consider the previous example, now with α_m = 0.4 and α_L = 0.8. In this case, the minimum stiffness ratio and minimum support diameter will be equal to 2.6cm and 45.9cm, respectively.

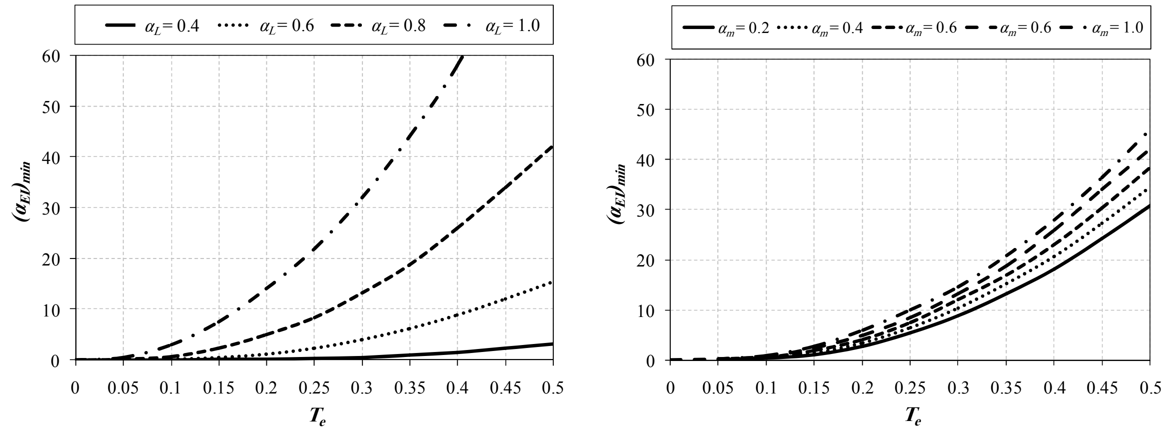

(a) Effect of height ratio (α_m = 0.8) (b) Effect of mass ratio (α_L = 0.8)

Fig. 5 Effect of height and mass ratios on minimum stiffness ratio

3.2 Effect of top and bottom masses

Effect of different top and bottom masses on minimum stiffness ratio is illustrated in Figs. 5,6. As it is clear from this figure, as the bottom mass of equipment increases the required stiffness ratio increases accordingly. There is a reverse trend for increasing top mass ratio i.e., the stiffness ratios decreases as the top mass of equipment increases. To illustrate the impact of top and bottom masses, consider previously mentioned example once with γ_b= 0.5 and another time with γ_t= 0.5 (α_m = α_L = 0.8). Based on calculations, minimum stiffness ratios corresponding to these systems will be equal to 8.55 and 0.8 which result the minimum support diameters equal to 68.2cm and 31.1cm, respectively.

As it can be deduced from Fig. 5 and Fig. 6, the general relationship between $(\alpha_{EI})_{min}$ and T_e can be well estimated using a second order polynomial model as it follows

$$(\alpha_{EI})_{\min} = q_1 T_e^2 + q_2 T_e + q_3, \qquad (\alpha_{EI})_{\min} \geq 0 \tag{11}$$

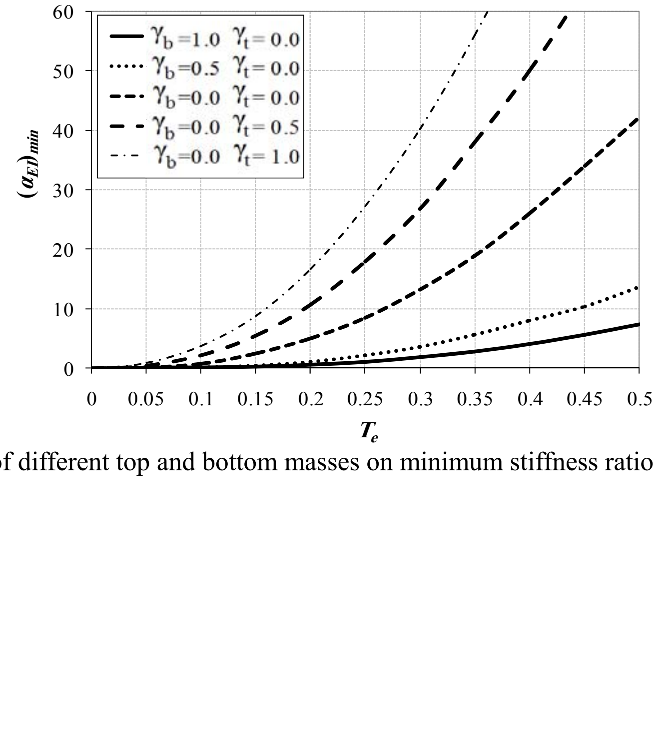

Fig. 6 Effect of different top and bottom masses on minimum stiffness ratio (α_m = α_L = 0.8)

Where, the coefficients q_1, q_2 and q_3 are given for different system properties in Table 1. Above expression has an acceptable degree of accuracy when the resultant $(\alpha_{EI})_{min}$ is more than unity (error < 5%). It should be noted that Table 1 is generated by analyzing 125,000 candlestick support-equipment sets with different system properties. Employing this table will help designers to control DAF of any candlestick support-equipment system easily. Fig. 7 displays a flowchart which can be used in evaluating DAF of supporting structures.

Table 1 Parameters of Eq. (11) for different system properties

		$\gamma_t=\gamma_b=0.0$			γ_t=0.0						γ_b=0.0					
α_m	α_L				γ_b=0.5			γ_b=1.0			γ_t=0.5			γ_t=1.0		
		q_1	q_2	q_3	q_1	q_2	q_3	q_1	q_2	q_3	q_1	q_2	q_3	q_1	q_2	q_3
	0.2	0.00	0.00	0.00	6.00	-2.82	0.39	10.00	-3.99	0.49	0.00	0.00	0.00	0.00	0.00	0.00
	0.4	31.00	-14.15	1.77	51.95	-13.17	1.00	69.12	-11.01	0.50	-12.00	11.40	-2.52	0.00	0.00	0.00
0.2	0.6	82.18	-20.35	1.39	145.40	-17.92	0.64	207.85	-16.62	0.38	33.00	-12.94	1.40	48.11	-32.50	5.58
	0.8	168.26	-24.36	1.01	330.42	-26.59	0.76	480.30	-25.84	0.78	73.50	-20.04	1.61	44.43	-14.36	1.26
	1.0	309.70	-28.76	0.90	613.64	-28.46	0.84	911.52	-34.11	1.91	122.68	-20.12	0.92	81.24	-19.16	1.34
	0.2	0.00	0.00	0.00	8.00	-4.40	0.70	10.57	-4.33	0.54	0.00	0.00	0.00	0.00	0.00	0.00
	0.4	32.19	-13.88	1.64	52.90	-13.22	1.01	70.74	-11.41	0.53	1.60	-0.13	-0.05	0.00	0.00	0.00
0.4	0.6	85.94	-19.35	1.23	146.87	-16.10	0.43	218.85	-19.02	0.56	35.05	-13.22	1.45	38.06	-22.39	3.42
	0.8	179.27	-21.82	0.72	339.52	-23.45	0.56	498.91	-26.97	0.89	73.37	-16.84	1.11	52.57	-18.03	1.86
	1.0	343.76	-26.54	0.86	652.73	-31.24	1.21	957.27	-38.43	2.49	133.14	-19.18	0.83	88.90	-18.73	1.18
	0.2	0.00	0.00	0.00	6.60	-3.13	0.43	11.29	-4.81	0.62	0.00	0.00	0.00	0.00	0.00	0.00
	0.4	32.52	-13.43	1.56	55.84	-14.14	1.09	69.83	-10.28	0.41	7.40	-4.25	0.70	0.00	0.80	-0.25
0.6	0.6	89.49	-18.68	1.14	149.16	-14.59	0.29	214.52	-15.14	0.26	34.88	-11.64	1.11	23.57	-10.25	1.18
	0.8	193.36	-21.19	0.69	360.30	-25.82	0.76	517.58	-30.10	1.24	76.60	-15.45	0.93	52.90	-15.70	1.40
	1.0	372.73	-24.25	0.99	676.97	-27.90	1.35	992.42	-40.89	2.94	149.21	-20.63	1.01	93.99	-17.22	1.03
	0.2	0.00	0.00	0.00	7.20	-3.67	0.56	11.00	-4.50	0.56	0.00	0.00	0.00	0.00	0.00	0.00
	0.4	34.05	-13.78	1.59	54.10	-12.37	0.86	74.47	-12.41	0.64	12.80	-8.32	1.48	0.00	0.92	-0.29
08	0.6	95.25	-18.86	1.10	161.80	-18.33	0.63	224.48	-17.23	0.42	36.86	-11.97	1.14	22.93	-9.00	0.95
	0.8	207.91	-20.31	0.66	357.21	-18.70	0.34	537.03	-31.73	1.38	79.68	-14.20	0.77	51.15	-12.84	1.01
	1.0	408.00	-17.77	0.73	700.30	-19.86	1.16	1018.12	-33.75	2.67	139.93	-8.67	-0.12	92.45	-10.63	0.26
	0.2	0.00	0.00	0.00	6.29	-2.83	0.38	10.64	-4.25	0.52	0.00	0.00	0.00	0.00	0.00	0.00
	0.4	38.29	-15.66	1.82	55.48	-12.70	0.90	73.50	-11.23	0.51	12.57	-7.42	1.20	3.60	-2.26	0.43
1.0	0.6	97.25	-17.29	0.93	158.79	-14.47	0.26	223.58	-15.00	0.28	38.75	-11.98	1.10	21.71	-7.63	0.77
	0.8	214.97	-16.86	0.51	375.33	-20.08	0.52	528.18	-20.83	0.69	82.39	-13.02	0.65	51.64	-10.90	0.70
	1.0	444.42	-7.15	-0.07	762.73	-23.89	1.62	1066.67	-32.15	2.85	164.01	-10.81	0.12	100.62	-8.81	-0.04

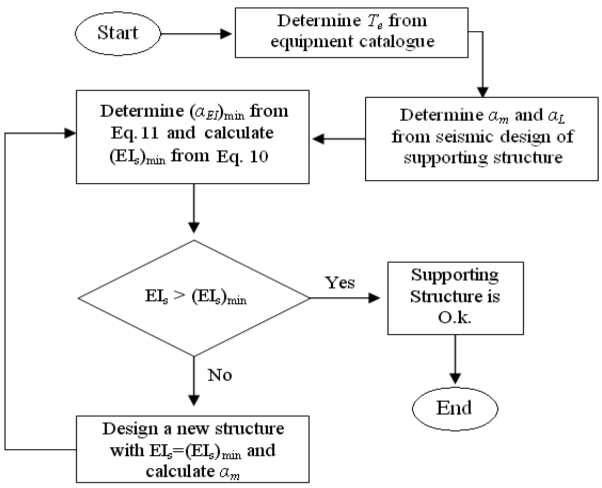

Fig. 7 Flowchart for evaluating DAF of supporting structure

4. Introduction to probabilistic evaluation of DAF

4.1 Uncertainty parameters

As it is described in the previous section, dynamic amplification factor of supporting structure may be calculated using Eq. 6. In this equation, $B(\omega_n, \xi)$ (from now on shown by B_n) is assumed to be deterministic parameter which can be calculated using Eq. (7). But as we know, different earthquakes have different spectral shapes (normalized response spectrum) and a structural system designed with a specific response spectrum may have completely different behaviour when subjected to another earthquake.

Fig. 8 displays mean and standard deviation of normalized response spectra for 2% damping, obtained from 20 earthquakes which are proposed by FEMA 440 (2005) for the site class C. As it is clear from this figure, the normalized response spectra have wide scatter around the mean value at all periods. Therefore, a structural system which its *DAF* is calculated using mean values, $\overline{B}_n$, (from now on shown by $\overline{DAF}$), will have different *DAF* when subjected to each of 20 earthquakes. This source of uncertainty in determining dynamic amplification of support structures can be accounted for by the means of probabilistic evaluation of *DAF*.

Although, there are other sources of uncertainty in structural modeling, structure loading, analyzing, etc. which can be accounted for in a probabilistic analysis, but their evaluation requires more study and is beyond the scope of this work.

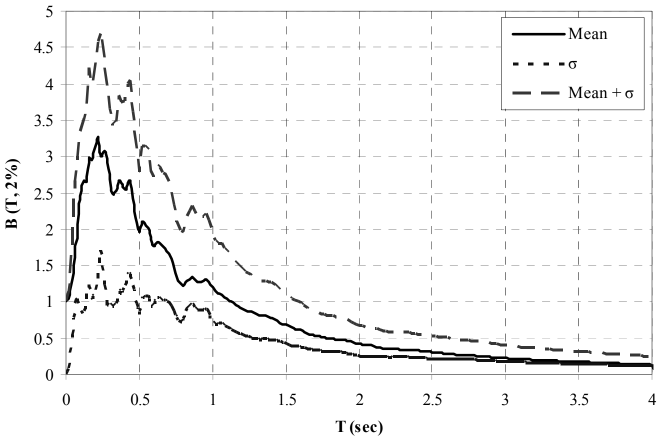

Fig. 8 Mean and standard deviation of records proposed by FEMA 440 for the site class C

4.2 Limit state function

Limit state function defines the border line (or surface) between the safe and unsafe states. This function may be defined with respect to different barriers. Regarding dynamic amplification of candlestick support structures, this function may be indicated as

$$g(X) = DAF_{all} - \sum_{n=1}^{N} \left| D_{1n} \times B_n \right| \tag{12}$$

Where $g(X)$ is the limit state function and DAF_{all} is the allowable dynamic amplification factor. Using this equation, one of the following conditions may occur:

$g(X) > 0$; safe state where DAF of supporting structure is less than allowable DAF.

$g(X) < 0$; failure state where DAF of supporting structure is more than allowable DAF.

$g(X) = 0$; limit state line (or surface).

Since Eq. (12) is a linear function of input random variables, the distribution type of input variables and limit state function will be identical. Distribution type of random variables B_1 to B_4, defines how the spectral accelerations of different earthquake records at a given period are distributed around the mean value. Generally, these variables may follow various distribution types but the case of normal and lognormal distributions are discussed herein.

4.3 Reliability calculation

Applying the expectation operator to both sides of Eq. (12), the mean value of limit state function can be indicated in the form

$$\mu_{g(X)} = DAF_{all} - \sum_{n=1}^{N} \left| D_{1n} \times \overline{B}_n \right| \tag{13}$$

Since, there is a linear combination between different uncertainty parameters (namely the parameter B_n, $n = 1, 2, 3, 4$) in Eq. (12), variance of limit state function will be equal to

$$\sigma^2_{g(X)} = \sum_{n=1}^{N} \left(D^2_{1n} \times \sigma^2_{B_n} \right) \tag{14}$$

Taking the mean and standard deviation of limit state function and assuming that the limit state function follows a normal distribution, the reliability index (β) can be calculated as

$$\beta = \mu_{g(X)} / \sigma_{g(X)} \tag{15}$$

Substituting Eqs. (13) and (14) in Eq. (15), the reliability index for passing the target DAF can be calculated as

$$\beta = \frac{DAF_{all} - \sum_{n=1}^{N} \left| D_{1n} \times \overline{B}_n \right|}{\sqrt{\sum_{n=1}^{N} \left(D^2_{1n} \times \sigma^2_{B_n} \right)}} \tag{16}$$

Using above equation, the probability of exceeding a specific DAF_{all} can be defined as

$$P_e = P\{g(X) \le 0\} = 1 - \Phi(\beta) \tag{17}$$

Where, $\Phi(-)$, is the cumulative distribution function of a normal variable. For lognormal distribution, the probability of exceeding DAF_{all} will be equal to:

$$P_e = P\{g(X) \le 0\} = 1 - \Gamma(DAF_{all}, \mu_{\log}, \sigma_{\log}) \tag{18}$$

Where, $\Gamma(-)$, is the cumulative distribution function of a lognormal variable. In above equation, μ_{log} and σ_{log} are the parameters of lognormal distribution function which can be calculated as

$$\mu_{\log} = Ln\left(\frac{\mu_{g(X)}^{2}}{\sqrt{\mu_{g(X)}^{2} + \sigma_{g(X)}^{2}}}\right) \quad (19)$$

$$\sigma_{\log} = \sqrt{Ln\left(\frac{\sigma_{g(X)}^{2}}{\mu_{g(X)}^{2}} + 1\right)} \quad (20)$$

4.4 Discussion on results

Having the mean and standard deviation of normalized response spectrum for a set of earthquakes, the parameters $\overline{B}_n$ and σ_{Bn} can be determined for each vibration mode. Using these values in conjunction with Eq. (17) or Eq. (18), the probability of exceeding a target DAF can be calculated for a candlestick support-equipment combination. Fig. 9 displays probability of exceeding different DAF barriers, for a candlestick support-equipment with $\alpha_m = \alpha_L = 0.8$, $\gamma_b = \gamma_t = 0$, $T_e = 0.25$sec and different stiffness ratios.

Fig. 9(a) is plotted using the spectral shape of IEEE STD 693, Eq. (7), as the mean normalized response spectrum ($\overline{B}_n = B(\omega_n, \xi)$) with a coefficient of variation (COV) equal to 0.1 ($\sigma_{Bn} = 0.1 \times B(\omega_n, \xi)$). In order to obtain a single point on each curve of this figure, a modal analysis is performed on a 4DOF system with prescribed properties and a selected α_{EI} value. Using natural frequencies of this 4DOF system, the value of mean spectral accelerations, $\overline{B}_n$, for different vibration modes and corresponding standard deviations, σ_{Bn}, are determined from Eq. (7) and finally the probability of exceedance is calculated from Eq. (17) (the same quantities obtained from Eq. (18) are displayed with gray curves). In this figure, for $DAF_{all} = 2.25$ the stiffness ratio corresponding to 50% probability of exceedance is the one previously obtained for a similar support-equipment system and given in Table 1 ($\alpha_{EI} = 8.4$). This is because the stiffness ratios listed in Table 1 are adjusted to $DAF_{all} = 2.25$. For a similar support-equipment combination, the curve corresponding to $DAF_{all} = 2.5$ is also plotted in this figure. As it was mentioned before, this target DAF is the recommended scaling factor in IEEE STD 693 for qualification of equipment without supporting structure. As it is illustrated in Fig. 9(a), the probability of exceedance corresponding to the same stiffness ratio ($\alpha_{EI} = 8.4$) is about 5%.

Same plots with COV = 0.15 and COV = 0.2 are presented in Fig. 9(b) and Fig. 9(c), respectively. It can be inferred from these figures that as the COV of input variables increases, the probability of exceeding $DAF_{all} = 2.5$ increases accordingly. This means that for a substation site with large differences in the spectral shape of historical earthquakes, exceeding the barrier $DAF_{all} = 2.5$ is more probable for supporting structures.

In preparation of Fig. 9(d), the parameters $\overline{B}_n$ and σ_{Bn} are taken from mean and standard deviation of earthquake records proposed by FEMA 440 for the site class C (Fig. 8). This figure illustrates a substantial decrease in probability of exceeding different DAF barriers. This is because the spectral shape of IEEE STD 693 is intended to envelop a large number of anticipated earthquakes and has a flat plateau over a wide range of frequencies (see Fig. 3). On the other hand, the mean normalized response spectrum given in Fig. 8 reflects characteristics of limited number of real earthquakes and thus has a smaller flat plateau. As it can be seen from Fig. 9(d), the probability of exceeding $DAF_{all} = 2.5$ for a support structure with $\alpha_{EI} = 8.4$ subjected to 20 prementioned earthquake records, is about 3.5% which is close to what observed in Fig. 9(a) assuming COV = 0.1.

For candlestick support-equipment systems listed in Table 1 ($\gamma_t = \gamma_b = 0$), the probability of exceedance is calculated for DAF_{all} = 2.5 using the spectral shape of Eq. (7) as the mean normalized response spectrum with COV = 0.1 and results are given in Table 2. As it can be seen in this table, for different support-equipment combinations probability of exceeding DAF_{all} = 2.5, varies from 3.65% to 9.25%. Therefore, it can be said that for a support-equipment system which its DAF is controlled using the minimum stiffness ratios given in Table 1, there will be only about 4-9% probability of not being qualified Using IEEE STD 693 specifications.

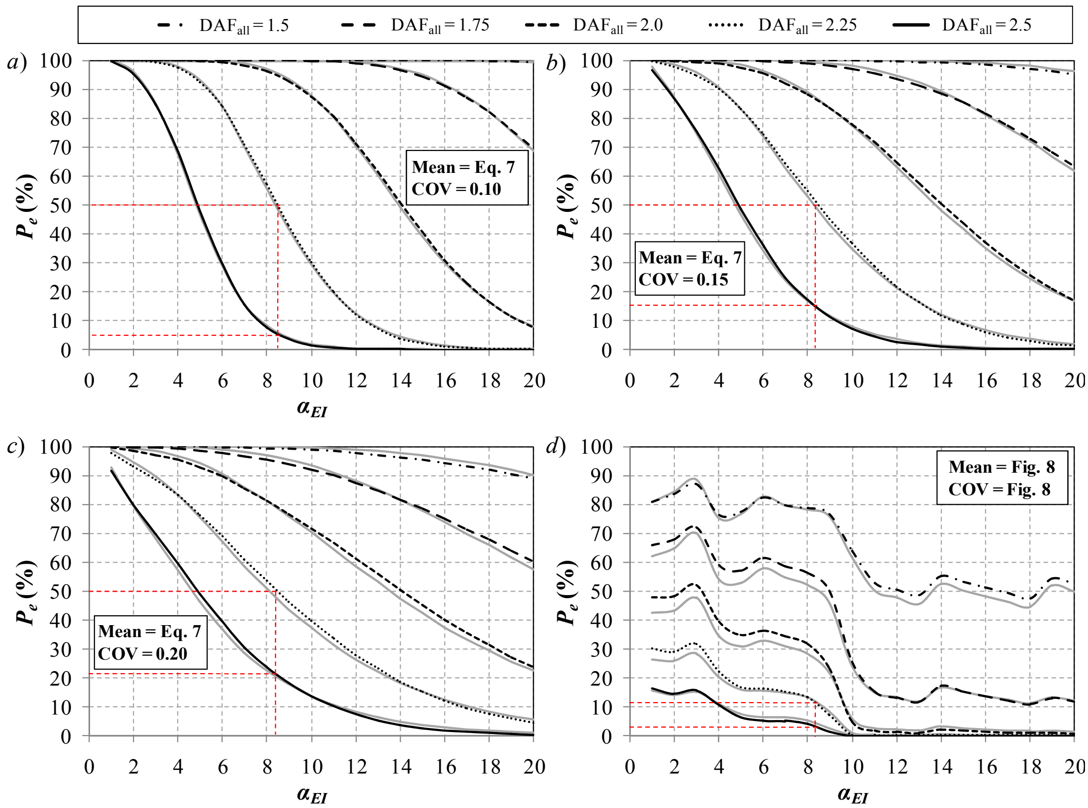

Fig. 9 Probability of exceeding different DAF barriers, for a candlestick support-equipment with $\alpha_m = \alpha_L = 0.8$, $\gamma_b = \gamma_t = 0$, $T_e = 0.25$sec

Table 2 Probability of exceeding DAF_{all} = 2.5 for candlestick support-equipment combinations listed in Table 1 ($\gamma_t = \gamma_b = 0$)

α_m	α_L	T_e									
		0.05	0.10	0.15	0.20	0.25	0.30	0.35	0.40	0.45	0.50
	0.2	0.00	0.00	0.00	0.00	0.00	0.00	8.67	7.49	6.66	6.26
0.2	0.4	0.00	0.00	6.92	6.87	5.90	4.47	4.27	4.25	4.68	4.90
	0.6	5.92	5.34	4.42	4.59	4.06	4.62	4.37	5.30	6.19	5.77

Table 2 Continued

0.2	0.8	6.60	5.96	5.57	4.12	4.36	5.52	6.03	6.71	7.00	7.47
	1.0	7.24	6.30	5.21	5.18	5.44	6.31	6.89	7.71	8.01	7.84
0.4	0.2	0.00	0.00	0.00	0.00	0.00	9.13	8.51	7.43	6.93	6.86
	0.4	0.00	0.00	6.61	6.08	4.61	4.27	4.21	4.25	4.95	4.14
	0.6	6.52	5.68	4.71	4.42	4.69	3.80	4.85	5.56	5.61	6.21
	0.8	7.18	6.65	5.66	4.64	4.84	5.43	6.24	7.27	7.70	7.84
	1.0	7.91	6.07	5.69	5.48	4.66	6.21	6.76	8.19	8.64	7.46
0.6	0.2	0.00	0.00	0.00	0.00	0.00	8.12	8.05	7.56	7.34	6.06
	0.4	0.00	6.71	6.46	5.54	3.91	4.29	4.31	3.65	4.93	4.93
	0.6	6.38	6.21	5.17	3.73	4.41	4.52	5.28	5.88	6.93	6.62
	0.8	6.97	5.59	5.61	5.15	5.28	5.32	7.00	7.93	7.87	8.18
	1.0	7.30	6.03	4.89	5.47	6.43	7.24	8.24	8.93	8.46	9.10
08	0.2	0.00	0.00	0.00	0.00	0.00	9.25	8.21	6.33	6.39	6.88
	0.4	0.00	6.93	5.46	5.43	5.11	4.45	4.49	4.81	5.20	5.52
	0.6	5.65	6.12	5.06	5.18	5.12	5.24	5.68	6.24	6.30	6.99
	0.8	7.17	6.31	4.71	4.49	5.67	6.51	7.68	6.98	7.19	8.48
	1.0	8.85	6.04	4.89	4.76	6.32	7.76	8.50	9.16	7.60	8.04
1.0	0.2	0.00	0.00	0.00	0.00	0.00	9.13	6.96	6.06	7.05	6.51
	0.4	0.00	5.24	5.73	5.46	4.88	4.72	4.74	4.95	5.46	4.33
	0.6	6.38	6.23	5.27	5.23	4.96	4.50	6.04	6.56	7.52	7.32
	0.8	6.16	6.67	5.45	4.39	5.01	7.20	7.67	8.50	8.96	8.74
	1.0	8.77	6.09	4.81	5.63	6.12	6.78	7.24	8.08	8.98	7.95

5. Conclusions

In this paper a parametric study is implemented in order to improve seismic design of substation structures. In the first phase of study, dynamic amplification factor (DAF) of different candlestick support-equipment combinations is evaluated and compared to the target DAF presented in IEEE STD 693. Based on this procedure, a minimum stiffness ratio is obtained for each candlestick support-equipment combination which guarantees that the supporting structure will not amplify the ground motions more than 2.25 times when subjected to an IEEE STD 693 compatible earthquake. In the second part, a probabilistic framework is utilized in order to account for uncertainties inherent in spectral shape of different earthquakes. Using the spectral shape of IEEE STD 693 as the mean normalized response spectrum and assuming different coefficients of variation, the probability of exceeding DAF = 2.25 and DAF = 2.5 is calculated for different candlestick support-equipment combinations and compared. Also, this is done using the mean and standard deviation of earthquake records proposed by FEMA440 for the site class C. Based on the results, for a support-equipment system which is designed to satisfy DAF = 2.25 criterion, there is only 4-9% probability of not satisfying DAF = 2.5 criterion. Application of the results presented in this paper in conjunction with a seismic design code, can result in seismic resistant support-equipment combinations and decrease the earthquake induced damages to substations.

References

Architectural Institute of Japan (AIJ) (1998), *Investigation Report on the Great Hanshin-Awaji Earthquake*,

Volume 3: Urban Disaster Prevention System, Marusen Corp. Press, Tokyo, Japan.
ASCE Guide (1996), *Guide to Improved Earthquake Performance of Electric Power Systems*, ASCE Manuals and Reports on Engineering Practice No. 96.
ASCE Manual (2008), *Substation Structures Design Guide*, ASCE Manuals and Reports on Engineering Practice No. 113.
ASCE-TCLEE (1997), *Northridge Earthquake: Lifeline performance and post earthquake response*, American Society of Civil Engineering Technical Council on Life Line Earthquake Engineering.
Clough, R.W. and Penzien, J. (1993), *Dynamics of Structures*, 3rd Ed., McGraw-Hill Publishing Company, New York.
Chang, L. and Wu, Z. (2011), "Performance and reliability of electrical power grids under cascading failures", *Int. J. Elec. Power Energy Syst*., **33**(8), 1410-1419.
Chopra, A.K. (2007), *Dynamics of Structures; Theory and Application to Earthquake Engineering*, 3rd Edition, Prentice Hall.
Dastous, J.B., Filiatrault, A. and Pierre, J.R. (2004), "Estimation of displacement at interconnected points of substation equipment subjected to earthquake", *IEEE Trans. Power Del*., **19**(2), 618-628.
Dastous, J.B. (2007), "Guidelines for seismic design of flexible buswork between substation equipment", *Earthq. Eng. Struct. Dyn*., **36**, 191-208.
Dastous, J.B. and Pierre, J.R. (2007), "Design methodology for flexible buswork between substation equipment subjected to earthquake", *IEEE Trans. Power Del*., **22**(3), 1490-1497.
Feizi, B., Saadeghvaziri, M.A., Ersoy, S. and Ashrafi, A. (2008), *Seismic Evaluation and Rehabilitation of Critical Electric Power System Components*, Department of Civil and Environmental Engineering, New Jersey Institute of Technology, Newark, NJ 07102.
FEMA 440 (2005), *Improvement of Nonlinear Static Seismic Analysis Procedures*, Federal Emergency Management Agency (FEMA), Washington, D.C..
Gilani, A.S., Whittaker, A.S., Fenves, G.L. and Chen, C. (2000), *Seismic Evaluation and Analysis of 230-kV Disconnect Switches*, PEER Report 2000/06, University of California, Berkeley.
Hatami, M., Ghafory-ashtiani, M. and Hosseini, M. (2004), "Experimental and analytical study of a high voltage instrument transformer", *13th World Conference on Earthquake Engineering*, Vancouver, B.C., Canada.
IEEE Standard 693 (2006), *IEEE Recommended Practice for Seismic Design of Substations*, IEEE, 3 Park Avenue, New York, NY 10016-5997, USA.
Matt, H. and Filiatrault, A. (2004), *Seismic Qualification Requirements for Transformer Bushings*, Department of Structural Engineering University of California, San Diego La Jolla, California 92093-0085.
Pham, T. (2005), *Two-Dimensional Shaking Table Test of Transformer Bushing with Seismic Isolation Device*, MCEER Report, Department of civil and environmental Engineering, University of California at Irvin.
Shinozuka, M., Dong, X., Chen, T.C. and Jin, X. (2007), "Seismic performance of electric transmission network under component failures", *Earthq. Eng. Str. Dyn*., **36**(2), 227-244.
Takhirov, S.M., Fenves, G.L. and Fujisaki, E. (2005), *Seismic Qualification and Fragility Testing of Line Break 550 kV Disconnect Switches*, PEER Report, University of California, Berkeley.
Wen, B. and Niu, D. (2011), "Seismic response analysis of substation involving interaction of main structure-electrical equipment", *Adv. Mat. Res*., **163-167**, 4022-4026.